



## OPEN ACCESS

# Fluorescent TEM-1 $\beta$ -lactamase with wild-type activity as a rapid drug sensor for *in vitro* drug screening

Wing-Lam Cheong\*, Ming-San Tsang\*, Pui-Kin So\*, Wai-Hong Chung\*, Yun-Chung Leung\* and Pak-Ho Chan\*<sup>†1</sup>

\*State Key Laboratory of Chirosciences, Food Safety and Technology Research Centre, Department of Applied Biology and Chemical Technology, The Hong Kong Polytechnic University, Hung Hom, Kowloon, Hong Kong, People's Republic of China

<sup>†</sup>The Hong Kong Polytechnic University Shenzhen Research Institute, Shenzhen 518057, People's Republic of China

## Synopsis

We report the development of a novel fluorescent drug sensor from the bacterial drug target TEM-1  $\beta$ -lactamase through the combined strategy of Val<sup>216</sup>→Cys<sup>216</sup> mutation and fluorophore labelling for *in vitro* drug screening. The Val<sup>216</sup> residue in TEM-1 is replaced with a cysteine residue, and the environment-sensitive fluorophore fluorescein-5-maleimide is specifically attached to the Cys<sup>216</sup> residue in the V216C mutant for sensing drug binding at the active site. The labelled V216C mutant has wild-type catalytic activity and gives stronger fluorescence when  $\beta$ -lactam antibiotics bind to the active site. The labelled V216C mutant can differentiate between potent and impotent  $\beta$ -lactam antibiotics and can distinguish active-site binders from non-binders (including aggregates formed by small molecules in aqueous solution) by giving characteristic time-course fluorescence profiles. Mass spectrometric, molecular modelling and trypsin digestion results indicate that drug binding at the active site is likely to cause the fluorescein label to stay away from the active site and experience weaker fluorescence quenching by the residues around the active site, thus making the labelled V216C mutant to give stronger fluorescence in the drug-bound state. Given the ancestor's role of TEM-1 in the TEM family, the fluorescent TEM-1 drug sensor represents a good model to demonstrate the general combined strategy of Val<sup>216</sup>→Cys<sup>216</sup> mutation and fluorophore labelling for fabricating tailor-made fluorescent drug sensors from other clinically significant TEM-type  $\beta$ -lactamase variants for *in vitro* drug screening.

**Key words:** antibiotics, bacteria,  $\beta$ -lactamase, drug screening, inhibitors, sensor

Cite this article as: Cheong, W.-L., Tsang, M.-S., So, P.-K., Chung, W.-H., Leung, Y.-C. and Chan, P.-H. (2014) Fluorescent TEM-1  $\beta$ -lactamase with wild-type activity as a rapid drug sensor for *in vitro* drug screening. *Biosci. Rep.* **34**(5), art:e00136.doi:10.1042/BSR20140057

## INTRODUCTION

$\beta$ -Lactam antibiotics have been widely used as therapeutic agents in the treatment of bacterial infections. These drugs, which share a common structural characteristic of four-membered  $\beta$ -lactam ring, can irreversibly bind to the active site of penicillin-binding proteins, thus inhibiting these bacterial proteins from synthesizing cell walls and leading to cell death [1]. The overuse of  $\beta$ -lactam antibiotics in various areas (e.g. clinical treatment and animal farming), however, has led to a worrying worldwide clinical problem – the emergence of antibiotic-resistant bacteria. Many bacteria have developed an effective defence mechanism

against  $\beta$ -lactam antibiotics by producing  $\beta$ -lactamases, which are efficient enzymes capable of catalysing  $\beta$ -lactam hydrolysis [2,3]. The TEM family is classified as class A serine-type  $\beta$ -lactamase in which the Ser<sup>70</sup> residue in the active site is activated by Glu<sup>166</sup> to form Ser<sup>70-O<sup>-</sup></sup> (through the deprotonation of the side-chain –OH group), which subsequently opens the  $\beta$ -lactam ring through the acylation with the  $\beta$ -lactam carbonyl group [4]. TEM-1 is regarded as the ancestor of the TEM family and offers ampicillin resistance to pathogenic bacteria (e.g. 90% of ampicillin resistance to *Escherichia coli* [5]; ampicillin and penicillin resistance to *Haemophilus influenzae* and *Neisseria gonorrhoeae* [6]). To date, more than 100 TEM variants have been derived from TEM-1 through one or more amino acid mutations,

**Abbreviations:** BAEE, N<sup>ε</sup>-benzoyl-L-arginine ethyl ester; ES, enzyme-substrate; ES\*, covalent enzyme-substrate; ESI-MS, electrospray ionization mass spectrometry; ESBL, extended spectrum  $\beta$ -lactamase; IRT, inhibitor-resistant TEM; TIPP tetraiodophenolphthalein; TEM, transmission electron microscopy.

<sup>1</sup> To whom correspondence should be addressed (email: pak-ho.chan@polyu.edu.hk).

including clinically relevant ESBLs (extended spectrum  $\beta$ -lactamases) and IRT (inhibitor-resistant TEM)  $\beta$ -lactamases (<http://www.lahey.org/Studies/>). The emergence of such enzymes has compromised the clinical utility of a broad spectrum of  $\beta$ -lactam antibiotics, including penicillins, cephalosporins and  $\beta$ -lactamase inhibitors [2, 7–11]. At present, TEM variants (e.g. TEM-3, TEM-10, TEM-26 and TEM-52) are still widespread in many countries [9,10]. In view of this clinical threat, development of new and potent  $\beta$ -lactam antibiotics and non- $\beta$ -lactam inhibitors against TEM-type  $\beta$ -lactamases has been a very important research topic [12]. In recent years, the advent of computational drug screening has facilitated the discovery of new drug candidates through the high-throughput screening of compounds in chemical libraries *in silico* [13–16]. Despite this, *in vitro* drug screening is still an indispensable task because this study gives valuable experimental information on protein–drug binding in solution and the efficacy of drug candidates [17,18]. Nitrocefim, a colorimetric  $\beta$ -lactam antibiotic, has been routinely used to assess the inhibitory function of new drugs against  $\beta$ -lactamases [19]. This colorimetric antibiotic acts as a competitive binder to  $\beta$ -lactamases to probe the inhibitory activity of drug candidates; the enzymatic hydrolysis and subsequent coloured product formation (with strong absorbance at 482 nm) of nitrocefim will be reduced if the drug candidates can bind to the active site of  $\beta$ -lactamases, and vice versa. The nitrocefim method, however, is an indirect approach as it is unable to directly probe the binding interaction of drug candidates with the active site of  $\beta$ -lactamases. Probing  $\beta$ -lactamase–drug binding, in fact, provides valuable information for new drug development (e.g. the binding affinity of new  $\beta$ -lactam antibiotics/inhibitors and their inhibitory activities). Despite the clinical relevance of many TEM-type  $\beta$ -lactamases, no attempt has been made to develop drug sensors based on such important molecular drug targets. We reasoned that TEM-type  $\beta$ -lactamases can be converted into fluorescent drug sensors through site-specific cysteine incorporation and fluorescent modification for *in vitro* drug screening purposes. Unlike the construction of fluorescently labelled proteins as simple ligand-binding biosensors [20–26], the development of fluorescent drug sensors from TEM-type  $\beta$ -lactamases for *in vitro* drug screening is much more challenging because the catalytic activity of the modified  $\beta$ -lactamases must be largely conserved in order to mimic their wild-type form for drug testing purposes. In this regard, it is very critical to choose a suitable residue in the target protein structure (for cysteine replacement) that does not significantly interfere with the enzymatic activity but still allows the attached fluorescent probe to sense drug binding at the active site.

Herein, we describe the development of a rapid fluorescent drug sensor from the clinically relevant TEM-1  $\beta$ -lactamase for *in vitro* drug screening. We chose TEM-1 because this enzyme is regarded as the ancestor in the TEM family in which many ESBL and IRT variants have been derived through one or more amino acid mutations in TEM-1 [2,6,8,9]. Thus, TEM-1 represents a good protein model to demonstrate the general strategy for developing fluorescent drug sensors from other clinically relevant TEM-type  $\beta$ -lactamases. Our strategy is to replace the Val<sup>216</sup> residue in TEM-1 with a cysteine to produce the V216C mutant

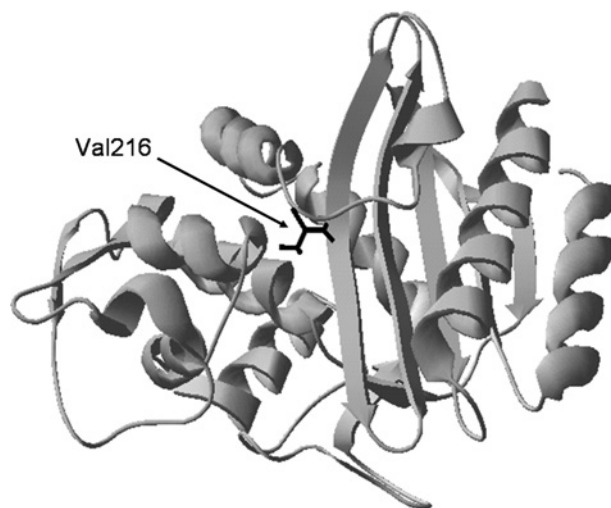


**Figure 1 Structure of the TEM-1  $\beta$ -lactamase**

The Val<sup>216</sup> residue is shown in black. The protein structure was constructed from TEM-1 (PDB code: 1ZG4).

and then covalently attach an environment-sensitive fluorescent probe (fluorescein-5-maleimide) to Cys<sup>216</sup> (through the formation of a thioether bond) for detecting drug binding at the active site [20,21]. The Val<sup>216</sup> residue was chosen because it is a non-catalytic residue which lies at the upper part of the active site (Figure 1). Thus, the replacement of Val<sup>216</sup> with a cysteine and the subsequent fluorophore labelling can largely conserve the catalytic activity of TEM-1, while the attached fluorophore can sensitively detect drug binding at the active site. This fluorescent TEM-1 V216C mutant with wild-type activity can mimic the catalytic behaviour of wild-type TEM-1, thus allowing itself to serve as an *in vitro* drug screening tool. More importantly, Val<sup>216</sup> is highly conserved in TEM-type  $\beta$ -lactamases. Thus, the combined strategy of Val<sup>216</sup>→Cys<sup>216</sup> mutation and fluorophore labelling represents a general approach to fabricating tailor-made fluorescent drug sensors from other clinically relevant TEM variants for *in vitro* drug-screening purposes.

## EXPERIMENTAL

### Chemicals and instruments

Penicillin G, ampicillin, cefoxitin (sodium salt), potassium clavulanate, BAEE (*N*<sup>c</sup>-benzoyl-L-arginine ethyl ester) hydrochloride, Congo red, 3',3'',5',5''-TIPP (tetraiodophenolphthalein), trypsin and aspirin were purchased from Sigma–Aldrich. Fluorescein-5-maleimide was purchased from Invitrogen. Fluorescence experiments were performed on a PerkinElmer LS-50B spectrofluorimeter. PerkinElmer Lambda 35 UV/VIS spectrophotometer was used for enzyme kinetic studies. ESI–MS (electrospray ionization mass spectrometry) experiments were conducted using a micromass Q-Tof-2<sup>TM</sup> spectrometer. CD measurements were

performed on a JASCO J-810 spectropolarimeter. TEM studies were performed using a DEOL JEM-2010 electron microscope.

### Protein expression and purification

*E. coli* BL21(DE3) was used as the bacterial strain to produce the wild-type and mutant (V216C) forms of the TEM-1  $\beta$ -lactamase. The proteins were (His)<sub>6</sub>-tagged at their C-terminus. The bacterial strain was incubated in 2 × TY medium overnight at 37 °C with shaking at 280 rev/min. A 2-ml portion of the overnight culture was then inoculated into 200 ml of sterile 2 × TY medium. The bacterial culture was further incubated at 37 °C with shaking at 280 rev/min. When OD<sub>600</sub> reached 0.8–0.9, IPTG (isopropyl  $\beta$ -D-thiogalactoside) was then added to the bacterial culture to induce protein expression. The bacterial culture was then incubated at 37 °C with shaking at 280 rev/min for another 6 h. The cell pellet was collected by centrifugation and then lysed by sonication. The proteins in the supernatant were purified by Ni<sup>2+</sup>-affinity chromatography with a linear gradient elution of 0–0.5 M imidazole in 20 mM sodium phosphate buffer (pH 7.0). The purified proteins were dialysed against deionized H<sub>2</sub>O at 4 °C, freeze-dried and stored at –20 °C. The purity of the proteins was examined by SDS/PAGE.

### Fluorophore labelling

The V216C mutant was labelled with fluorescein-5-maleimide. The protein was first dissolved in 6 ml of 50 mM potassium phosphate buffer (pH 7.0). A 5-fold molar excess of fluorescein-5-maleimide [20 mM, dissolved in DMF (dimethylformamide)] was then added to the protein solution, and the protein solution was stirred in dark at 25 °C for 30 min. After labelling, the protein solution was dialysed against deionized H<sub>2</sub>O at 4 °C and then freeze-dried.

### CD measurements

The far-UV CD spectra of the wild-type TEM-1 enzyme and the labelled and unlabelled V216C mutants were recorded using a JASCO J-810 spectropolarimeter. The wild-type TEM-1 enzyme and the labelled and unlabelled V216C mutants were dissolved in 50 mM potassium phosphate buffer (pH 7.0) to 5  $\mu$ M. The instrument was purged with nitrogen for 30 min before CD measurements. A quartz cuvette of 0.1-cm light absorption path length was used for far-UV (190–250 nm) CD measurements. The CD spectra were recorded in triplicate for each protein.

### Enzyme kinetics studies

The catalytic activities of the wild-type TEM-1 enzyme and the labelled and unlabelled V216C mutants were studied by the spectrophotometric method. The enzyme kinetics assays were performed with 10–1000  $\mu$ M penicillin G and ampicillin as the substrates in 50 mM potassium phosphate buffer (pH 7.0) at 20 °C. The hydrolytic reaction was initiated by mixing the enzymes with the substrates in a quartz cuvette of 1-cm light absorption path length. The UV absorbance of penicillin G and ampicillin were

then monitored at 233 and 235 nm, respectively, at each substrate concentration as a function of time. The initial rate for each substrate concentration was determined in duplicate by analysing the absorbance over the first 60 s. The initial rates were then fitted to the Hanes–Woolf equation to determine the  $k_{\text{cat}}$  and  $K_m$  values.

### Fluorescence measurements

The fluorescence of the labelled V216C mutant (20 nM) in the absence and presence of drug compounds (0, 0.01, 0.1 and 1 mM cefoxitin, penicillin G, ampicillin and clavulanate) in 50 mM potassium phosphate buffer (pH 7.0) was monitored using a PerkinElmer LS-50B spectrofluorimeter. A quartz cuvette of 1-cm light absorption path length was used for fluorescence measurements. The excitation and emission slit widths were 5 nm. The fluorescence signal of the labelled V216C mutant at 515 nm was recorded with excitation at 494 nm.

### MS studies

#### (a) Molecular mass measurements

The molecular masses of the wild-type TEM-1 enzyme and the labelled and unlabelled V216C mutants were determined by ESI-MS. Each of the proteins was dissolved in 150  $\mu$ l of 20 mM ammonium acetate buffer (pH 7.0) to a final concentration of 5–10  $\mu$ M. The protein solutions were centrifuged to remove insoluble materials. ESI-MS measurements were performed on a Micromass Q-ToF-2<sup>TM</sup> spectrometer. The protein samples were mixed with 1% formic acid dissolved in acetonitrile (1: 1, v/v) and injected into the electrospray source by a syringe pump (Harvard Apparatus, model 22) at a flow rate of 5  $\mu$ l min<sup>-1</sup>. The mass spectrometer was scanned over a range of 700–1600  $m/z$  and the multiply charged protein ion peaks were detected. The capillary and cone voltage were set at 3 kV and 30 V, respectively. Nitrogen was used as the desolvation, cone and nebulizing gas. The nebulizing gas was fully opened. The flow rates of the desolvation gas and cone gas were set at 400 and 50 L·h<sup>-1</sup>, respectively. The  $m/z$ -axis was calibrated externally with 10  $\mu$ M horse heart myoglobin ( $M_r = 16950.5$  Da). The raw multiply charged spectra were deconvoluted by the MassLynx 4.1 Transform Program.

#### (b) Detection of ES (enzyme–substrate) complexes

The formation of ES\* (covalent enzyme–substrate) complex during the course of hydrolytic reaction was probed by ESI-MS. A 200- $\mu$ l portion of the labelled V216C mutant (50  $\mu$ M) was added to 200  $\mu$ l of cefoxitin (100 mM), and the mixture was made up to 2000  $\mu$ l with 20 mM ammonium acetate solution (pH 7.0). At different time intervals, a 400- $\mu$ l portion of the reaction mixture was pipetted to 400  $\mu$ l of 20 mM ammonium acetate with 2% (v/v) formic acid to quench the hydrolytic reaction (pH ~2). The mixture was then concentrated and buffer-exchanged [20 mM ammonium acetate with 2% (v/v) formic acid] 1–2 times by means of Amicon<sup>®</sup> Ultra-15 (NMWL = 10 000) centrifugal filter devices (Millipore) to a final volume of about 150  $\mu$ l. ESI-MS measurements were then performed on a Micromass Q-ToF-2<sup>TM</sup>

spectrometer. Concentrated protein samples were mixed with 1 % formic acid dissolved in acetonitrile (1: 1 v/v) and injected into the electrospray source by a syringe pump (Harvard Apparatus, model 22) at a flow rate of  $5 \mu\text{l}\cdot\text{min}^{-1}$ . The mass spectrometer was scanned over a range of 700–1600  $m/z$ , and the multiply charged protein ion peaks were detected. The capillary and cone voltage were set at 3 kV and 30 V, respectively. Nitrogen was used as the desolvation, cone and nebulizing gas. The nebulizing gas was fully opened. The flow rates of the desolvation gas and cone gas were set at 400 and  $50 \text{L}\cdot\text{h}^{-1}$ , respectively. The  $m/z$ -axis was calibrated externally with  $10 \mu\text{M}$  horse heart myoglobin ( $M_r = 16950.5 \text{ Da}$ ). The raw multiply charged spectra were deconvoluted by the MassLynx 4.1 Transform Program.

### Molecular modelling studies

Molecular modelling of the labelled V216C mutant with and without penicillin G was performed using ICM-Pro 3.4-8a (Molsoft). The molecular model of the V216C mutant was constructed from the structure of TEM-1 (PDB: 1FQG). BPMC (Biased Probability Monte Carlo) minimization was used for energy minimization.

### TEM (transmission electron microscopy) measurements

TEM was used to examine the formation of ‘drug aggregates’ by small molecules under aqueous conditions. Samples of  $10 \mu\text{M}$  Congo red (dissolved in deionized water) and TIPP (dissolved in 0.5 % DMSO) were incubated with the labelled V216C mutant (20 nM). A drop of the solution mixture ( $10 \mu\text{l}$ ) was then applied onto a carbon grid (400 mesh), stained with 0.5 % PTA (phosphotungstic acid) and then dried overnight. TEM pictures were obtained with a 200 kV DEOL JEM-2010 electron microscope equipped with a Gatan MSC 794 CCD camera.

### Trypsin digestion studies

The labelled V216C mutant ( $0.2 \text{ mg}\cdot\text{ml}^{-1}$ ) was mixed with trypsin ( $0.01 \text{ mg}\cdot\text{ml}^{-1}$ ) in 50 mM potassium phosphate buffer (pH 7.0) in a quartz cuvette of 1-cm light absorption path length. The fluorescence spectra of the labelled V216C mutant were then recorded at various time intervals ( $t = 0, 2, 4, 6$  and 8 h) using a PerkinElmer LS50B spectrofluorimeter. The excitation wavelength was 460 nm, and the excitation and emission slit widths were 2.5 nm.

For SDS/PAGE analysis, the labelled V216C mutant ( $2 \text{ mg}\cdot\text{ml}^{-1}$ ) was mixed with trypsin ( $0.1 \text{ mg}\cdot\text{ml}^{-1}$ ) in 50 mM potassium phosphate buffer (pH 7.0) for 8 h. After digestion, a  $10\text{-}\mu\text{l}$  portion of the reaction mixture was collected and loaded onto a SDS/PAGE gel. The SDS/PAGE gel was illuminated with the UV light to obtain a fluorescent image. For comparison, a  $10\text{-}\mu\text{l}$  portion of the labelled V216C mutant ( $2 \text{ mg}\cdot\text{ml}^{-1}$ ) without trypsin digestion was also analysed in the same SDS/PAGE assay.

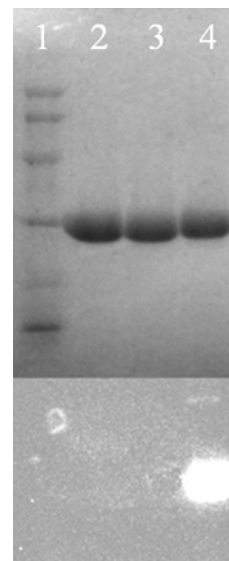


**Figure 2 SDS/PAGE analysis of the wild type and mutant forms of the TEM-1  $\beta$ -lactamase**

Lane 1 (protein markers): rabbit muscle phosphorylase b (97 400 Da), BSA (66 200 Da), hen egg white ovalbumin (45 000 Da), bovine carbonic anhydrase (31 000 Da), SBTI (soy-bean trypsin inhibitor, 21 500 Da), hen egg white lysozyme (14 400 Da); Lane 2: wild-type TEM-1; Lane 3: unlabelled V216C incubated with fluorescein (without the maleimide linker); Lane 4: labelled V216C. The fluorescent image (bottom) was obtained by illuminating the SDS/PAGE gel (top) with the UV light.

## RESULTS AND DISCUSSION

### Characterization of the labelled TEM-1 V216C mutant

The labelling reaction of the TEM-1 V216C mutant with the thiol-reactive fluorophore fluorescein-5-maleimide was monitored by SDS/PAGE. Briefly, wild-type TEM-1 and the V216C mutant were incubated with fluorescein-5-maleimide and then purified by dialysis to remove excess fluorophore. The protein samples were then loaded onto a SDS/PAGE gel for analysis. Figure 2 shows the protein bands for wild-type TEM-1 as well as the labelled and unlabelled V216C mutants. For the wild-type TEM-1 enzyme (without free cysteine), no observable fluorescent band appears upon illumination with the UV light (lane 2, Figure 2). In contrast, the labelled V216C mutant shows a strong fluorescent band (lane 4, Figure 2). These observations indicate that fluorescein-5-maleimide is specifically attached to the Cys<sup>216</sup> residue in the V216C mutant. In order to verify that the fluorescein molecule is covalently bound to the Cys<sup>216</sup> residue in the V216C mutant through the maleimide linker, a control experiment was performed in which the V216C mutant was incubated with fluorescein (without the maleimide linker) and then analysed by SDS/PAGE. In this case, the V216C mutant remains non-fluorescent (lane 3, Figure 2). This observation reveals that the fluorescein molecule is covalently bound to the Cys<sup>216</sup> residue through the thiol-reactive maleimide linker.

**Table 1** Steady-state kinetic parameters of the wild-type and mutant forms of the TEM-1  $\beta$ -lactamase

Form	$k_{\text{cat}}$ ( $\text{s}^{-1}$ )	$K_M$ (M)	$k_{\text{cat}}/K_M$ ( $\text{s}^{-1}\cdot\text{M}^{-1}$ )
Ampicillin			
Wild-type	$1040 \pm 34$	$(6.5 \pm 1.9) \times 10^{-5}$	$(1.6 \pm 0.5) \times 10^7$
V216C	$873 \pm 13$	$(1.4 \pm 0.1) \times 10^{-4}$	$(6.3 \pm 0.1) \times 10^6$
Labelled V216C	$650 \pm 58$	$(7.0 \pm 0.8) \times 10^{-4}$	$(9.2 \pm 1.9) \times 10^5$
Penicillin G			
Wild-type	$746 \pm 31$	$(1.3 \pm 0.2) \times 10^{-4}$	$(5.5 \pm 1.2) \times 10^6$
V216C	$491 \pm 13$	$(1.6 \pm 0.2) \times 10^{-4}$	$(3.0 \pm 0.4) \times 10^6$
Labelled V216C	$148 \pm 9$	$(2.6 \pm 0.4) \times 10^{-4}$	$(5.6 \pm 1.2) \times 10^5$

The labelled V216C mutant was further analysed by UV–Vis spectrophotometry. Supplementary Figure S1 (available at <http://www.bioscirep.org/bsr/034/bsr034e136add.htm>) shows the UV–Vis spectrum of the labelled V216C mutant. The labelled V216C mutant exhibits a visible absorption peak at 494 nm, which corresponds to the light absorption by fluorescein. This observation is consistent with the fact that the V216C mutant is covalently linked to fluorescein-5-maleimide after fluorophore labelling (Figure 2). To examine the extent of fluorophore labelling on the V216C mutant, we analysed the mass values of the V216C mutant before and after labelling with fluorescein-5-maleimide using ESI–MS. Supplementary Figure S2 (available at <http://www.bioscirep.org/bsr/034/bsr034e136add.htm>) shows the ESI mass spectra of the unlabelled and labelled V216C mutants. The unlabelled V216C mutant shows a mass peak of 29898 Da (Figure S2A). After labelling with fluorescein-5-maleimide, the V216C mutant gives a new mass peak of 30324 Da (Figure S2B). The mass difference between the labelled and unlabelled V216C mutants is 426 Da, which is close to the molecular mass of fluorescein-5-maleimide (427 Da). Furthermore, no significant mass peak appears at 29898 Da (corresponding to the unlabelled V216C mutant) in the mass spectrum of the labelled V216C mutant, indicating that the V216C mutant is completely labelled with fluorescein-5-maleimide (Figure S2B).

Far-UV CD measurements were performed on wild-type TEM-1 as well as the unlabelled and labelled V216C mutants. Supplementary Figure S3 (available at <http://www.bioscirep.org/bsr/034/bsr034e136add.htm>) shows the resulting far-UV CD spectra. In all cases, the CD spectra show strong peaks at 210 and 220 nm, which are characteristic of  $\alpha$ -helical structure (Figure S3). The CD signal for the labelled V216C mutant is very similar to those of the unlabelled V216C mutant and wild-type TEM-1, indicating that the secondary structure of the labelled V216C mutant is virtually similar to those of the unlabelled mutant and wild-type TEM-1.

### Enzyme kinetics studies

The catalytic activities of wild-type TEM-1 as well as the unlabelled and labelled V216C mutants were investigated by the spectrophotometric method [27–29]. With ampicillin as the substrate, the  $k_{\text{cat}}$  value for the unlabelled V216C mutant is similar to that of wild-type TEM-1, indicating that the V216C mutant

has similar catalytic activity to wild-type TEM-1 after the V216C mutation (Table 1). Interestingly, the labelled V216C mutant also has similar catalytic activity compared to the wild-type TEM-1 enzyme (similar  $k_{\text{cat}}$ ) even though the mutant carries the fluorescein molecule at its active site (Table 1). Similar observations were also obtained with penicillin G as the substrate. In all cases, the  $k_{\text{cat}}$  values for the unlabelled and labelled V216C mutants and the wild-type TEM-1 enzyme are within the same order of magnitude (Table 1). Unlike the case of removing catalytic residues (e.g. Glu<sup>166</sup>) in class A  $\beta$ -lactamases, which results in more than 1000-fold decrease in  $k_{\text{cat}}$  [21,27,30], the replacement of Val<sup>216</sup> with a cysteine in the TEM-1 structure does not significantly impair the catalytic activity of the enzyme. This phenomenon can be attributed to the fact that the Val<sup>216</sup> residue at the upper part of the active site is not directly involved in the catalytic process. Thus, the V216C mutation and the subsequent fluorophore labelling allow the catalytic activity of the labelled V216C mutant to be largely conserved with respect to that of the wild-type TEM-1 enzyme. With its conserved catalytic activity, the labelled V216C mutant can mimic the natural drug target, the wild-type TEM-1 enzyme, for *in vitro* drug screening purposes.

### Fluorescence response of the labelled V216C mutant to drug binding

The ability of the labelled V216C mutant to perform *in vitro* drug screening was investigated by fluorescence spectroscopy. The  $\beta$ -lactam antibiotics and  $\beta$ -lactamase inhibitor (clavulanate) used in this study are shown in Figure 3. We examined the fluorescence response of the labelled V216C mutant with cefoxitin, which is a cephalosporin antibiotic with strong resistance to the hydrolytic activity of TEM-1 [31–33]. Figure 4(A) shows the fluorescence signals of the labelled V216C mutant at different time intervals with different concentrations of cefoxitin. In the absence of cefoxitin, the labelled V216C mutant does not show significant fluorescence changes over the time course (Figure 4A). Upon addition of cefoxitin, the fluorescence of the labelled V216C mutant increases as a function of time and then becomes sustained (Figure 4A). Moreover, the fluorescence enhancement of the labelled V216C mutant increases with the concentration of cefoxitin (Figure 4A).

The fluorescence response of the labelled V216C mutant with less-resistant  $\beta$ -lactam antibiotics was also studied. Figure 4(B)

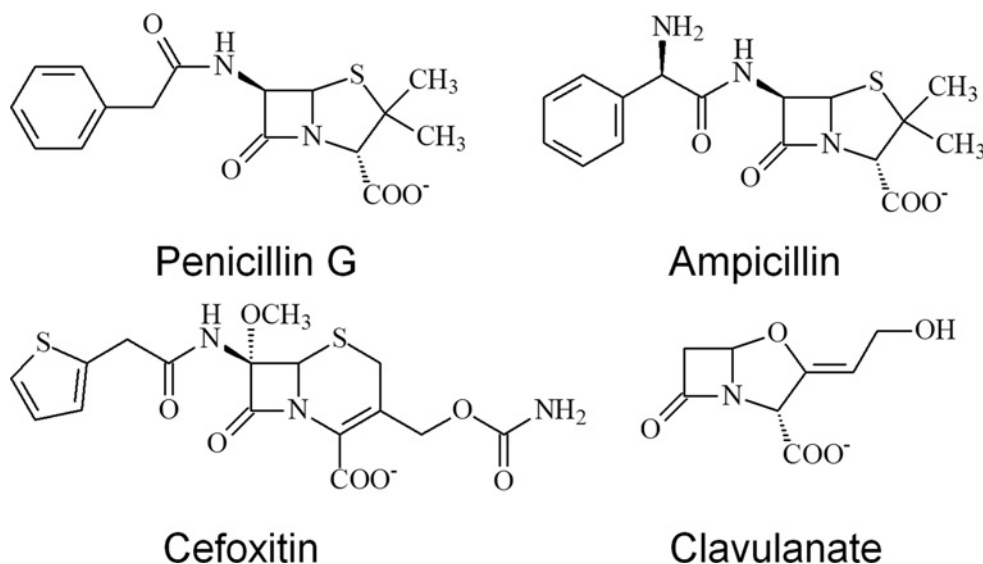


**Figure 3** Chemical structures of the  $\beta$ -lactam antibiotics and  $\beta$ -lactamase inhibitor used in this study

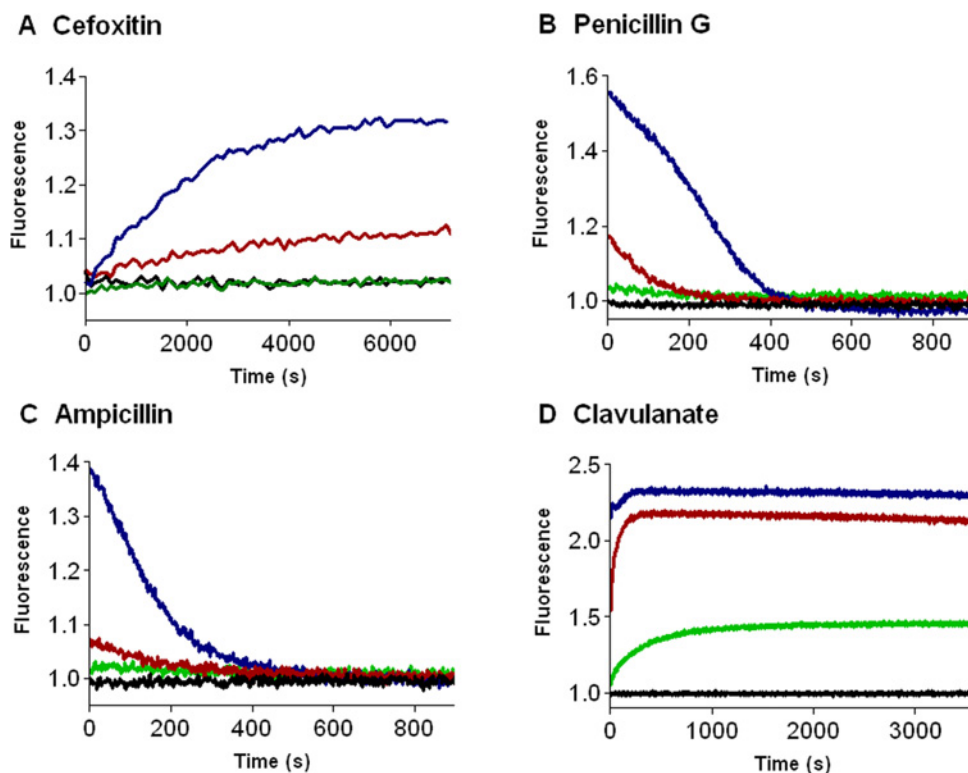


**Figure 4** Time-course fluorescence measurements of the labelled V216C mutant with different concentrations of  $\beta$ -lactam antibiotics and  $\beta$ -lactamase inhibitor

(A) cefoxitin; (B) penicillin G; (C) ampicillin; (D) clavulanate. The concentrations of the  $\beta$ -lactam antibiotics and  $\beta$ -lactamase inhibitor are shown in different colours: 0 mM (black), 0.01 mM (green), 0.1 mM (red), and 1 mM (blue). The labelled V216C mutant (20 nM) was dissolved in 50 mM potassium phosphate buffer (pH 7.0).

shows the fluorescence signals of the labelled V216C mutant with penicillin G at different time intervals. Without penicillin G, the labelled V216C mutant just gives steady and weak fluorescence over the time course (Figure 4B). In the presence of penicillin G (1 mM), the fluorescence of the labelled V216C mutant increases instantaneously and then declines (Figure 4B). With a lower concentration of penicillin G (0.1 mM), the fluorescence signal of the labelled V216C mutant also increases instantaneously (but to a smaller extent) and then decreases gradually (Figure 4B). Similar fluorescence measurements were also performed on the labelled V216C mutant with ampicillin. As similar to the case of penicillin G, the fluorescence of the labelled V216C mutant increases rapidly at the initial stage and then declines gradually over the time course (Figure 4C). The fluorescence response of the labelled V216C mutant towards clavulanate was also investigated. Clavulanate is an effective inhibitor against many class A  $\beta$ -lactamases [31,32]. This inhibitor can irreversibly bind to the active site of class A  $\beta$ -lactamases to form a stable covalent complex, resulting in the inhibition of enzymatic hydrolysis [31,34,35]. The fluorescence signals of the labelled V216C mutant in the presence of different concentrations of clavulanate are shown in Figure 4(D). In the absence of clavulanate, the labelled V216C mutant does not show significant fluorescence changes over the time course (Figure 4D). Upon addition of clavulanate (0.01 mM), the fluorescence of the labelled V216C mutant increases as a function of time and then becomes sustained (Figure 4D). The labelled V216C mutant gives stronger fluorescence in the presence of higher concentrations of clavulanate (0.1 and 1 mM) (Figure 4D).

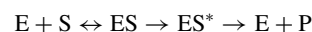
The specificity of the labelled V216C mutant was then examined. To this end, the fluorescence response of the labelled V216C mutant with non-binders (e.g. aspirin and BAEE) was monitored. As shown in Supplementary Figure S4 (available at <http://www.bioscirep.org/bsr/034/bsr034e136add.htm>), the fluorescence signals of the labelled V216C mutant with these non-binders remain virtually unchanged over the time course, unlike the cases of drug binders (e.g. cefoxitin, penicillin G, ampicillin and clavulanate; Figures 4A–D). These observations highlight the ability of the labelled V216C mutant to specifically recognize drug candidates capable of binding to the active site. The ability of the labelled V216C mutant to distinguish drug binders from ‘drug aggregates’ was also studied. Recent studies have shown that drug compounds selected *in silico* may form aggregates in aqueous solution [17, 36–39]. Such ‘drug aggregates’ can inhibit  $\beta$ -lactamase activity *in vitro* through non-specific mechanisms (e.g. protein adsorption/absorption), thus leading to hitting false-positive drug compounds in drug screening [17, 36–39]. To investigate whether the labelled V216C mutant can distinguish drug binders from ‘drug aggregates’, we studied the fluorescence response of the labelled V216C mutant in the presence of the aggregates formed by Congo red and TIPP. In aqueous solution, Congo red and TIPP tend to form aggregates, as revealed by the TEM images (Supplementary Figure S5 available at <http://www.bioscirep.org/bsr/034/bsr034e136add.htm>). Unlike the cases of drug binders (cefoxitin, penicillin G, ampicillin and clavulanate; Figures 4A–D), the labelled V216C mutant does not show significant fluorescence changes with the aggreg-

ates formed by Congo red (Supplementary Figure S6A available at <http://www.bioscirep.org/bsr/034/bsr034e136add.htm>) and TIPP (Figure S6B). These observations indicate that the labelled V216C mutant can distinguish active-site-binding drugs from ‘drug aggregates’ *in vitro*.

Taking all the fluorescence results together, the labelled V216C mutant can specifically detect drug binders capable of binding to the active site and eliminate non-binders and ‘drug aggregates’ in *in vitro* drug screening. Furthermore, the labelled V216C mutant can differentiate  $\beta$ -lactamase-resistant antibiotics/inhibitors (e.g. cefoxitin and clavulanate) from  $\beta$ -lactamase-unstable antibiotics (e.g. penicillin G and ampicillin) by giving characteristic fluorescence profiles (Figure 4). These interesting observations highlight the potential use of the labelled V216C mutant as a rapid drug sensor for *in vitro* drug screening in the development of new  $\beta$ -lactam antibiotics/inhibitors.

### Turn-on effect of drug binding on the labelled V216C mutant

To investigate the origin of the fluorescence changes of the labelled V216C mutant, the catalytic reaction of the labelled V216C mutant with cefoxitin was analysed by ESI-MS. Class A  $\beta$ -lactamases (including TEM enzymes) catalyse the hydrolysis of  $\beta$ -lactam antibiotics according to the three-step model (below) (where E is the free enzyme, S is a substrate, ES is a non-covalent enzyme-substrate complex, ES\* is a covalent enzyme-substrate complex, and P is the product) [40]:



Thus, by addition of an acid to denature TEM-1 at different time intervals, the catalytic reaction will be quenched and therefore the free enzyme (E) and the ES\* complex can be probed over the time course. In this MS study, we chose cefoxitin as the substrate because it is resistant to the hydrolytic action of TEM-type  $\beta$ -lactamases and can therefore form a stable ES\* complex in which the hydroxyl group of Ser<sup>70</sup> in the active site is covalently linked to the  $\beta$ -lactam carbonyl carbon with the aid of the activating residue Glu<sup>166</sup> [31,33]. The resulting ES\* complex is long-lived and can therefore be easily probed by ESI-MS. Supplementary Figure S7 (available at <http://www.bioscirep.org/bsr/034/bsr034e136add.htm>) shows the ESI mass spectra of the labelled V216C mutant with cefoxitin at different time intervals. The mass peaks A and B correspond to the free labelled V216C mutant (E) and the ES\* complex, respectively. The relative population of ES\* ( $[ES^*]/[E_{total}]$ , where  $[E_{total}] = [E] + [ES^*]$ ) at each time interval was then determined. The relative ES\* population increases as a function of time, indicating that the ES\* complex accumulates over the time course (rectangle, Figure 5). The relationship of the ES\* formation with the fluorescence change of the labelled V216C mutant was further investigated. To this end, the fluorescence of the labelled V216C mutant with cefoxitin was monitored at different time intervals under the solution conditions for the ESI-MS measurements ( $[labelled\ V216C] = 5\ \mu M$ ;  $[cefoxitin] = 10\ mM$ ;  $20\ mM$

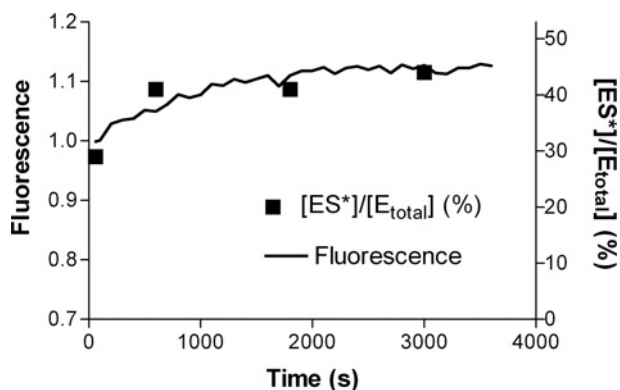


**Figure 5 Time-course ESI-MS and fluorescence measurements on the binding of the labelled V216C mutant to cefoxitin**

The time-course fluorescence profile of the labelled V216C mutant and the  $[ES^*]/[E_{total}]$  values measured by ESI-MS at different time intervals are shown in a solid line and black squares, respectively. The reaction of the labelled V216C mutant with cefoxitin took place in 20 mM ammonium acetate solution (pH 7.0).  $[Labelled\ V216C] = 5\ \mu M$ ;  $[Cefoxitin] = 10\ mM$ .

ammonium acetate, pH 7.0). Under such conditions, the fluorescence of the labelled V216C mutant increases as a function of time (Figure 5). Interestingly, the increasing fluorescence profile of the labelled V216C mutant is consistent with the increasing mass spectrometric profile of  $ES^*$ , indicating that the fluorescence enhancement of the labelled V216C mutant arises from the formation of  $ES^*$  complex (Figure 5).

We tried to probe the  $ES^*$  complexes of the labelled V216C mutant with penicillin G and ampicillin by ESI-MS. However, the reaction was so fast under the solution conditions for ESI-MS measurements that the  $ES^*$  complexes could not be traced. In order to unravel the origin of the initial fluorescence enhancements and the subsequent fluorescence declines of the labelled V216C mutant with penicillin G and ampicillin (Figures 4B–4C), we performed time-course UV absorbance measurements on these antibiotics and then compared these results with the time-course fluorescence profiles of the labelled V216C mutant. For penicillin G, the UV absorbance at 233 nm decreases as a function of time due to the enzymatic hydrolysis of the  $\beta$ -lactam ring (Supplementary Figure S8A available at <http://www.bioscirep.org/bsr/034/bsr034e136add.htm>). The hydrolytic reaction is virtually complete after 500 s. Interestingly, the fluorescence of the labelled V216C mutant is enhanced instantaneously upon addition of penicillin G and then declines gradually in a similar time interval ( $\sim 500$  s) (Figure S8B). For ampicillin, the fluorescence of the labelled V216C mutant and the UV absorbance of ampicillin both decrease in a similar time interval ( $\sim 400$  s) (Supplementary Figure S9A–9B available at <http://www.bioscirep.org/bsr/034/bsr034e136add.htm>). These observations indicate that the labelled V216C mutant gives stronger fluorescence upon binding to penicillin G and ampicillin to form  $ES^*$  complexes and then restores its weak fluorescence as a result of the release of the hydrolysed products ( $ES^* \rightarrow E + P$ ).

In order to examine the effect of drug binding at the active site on the conformation of the attached fluorescein molecule,

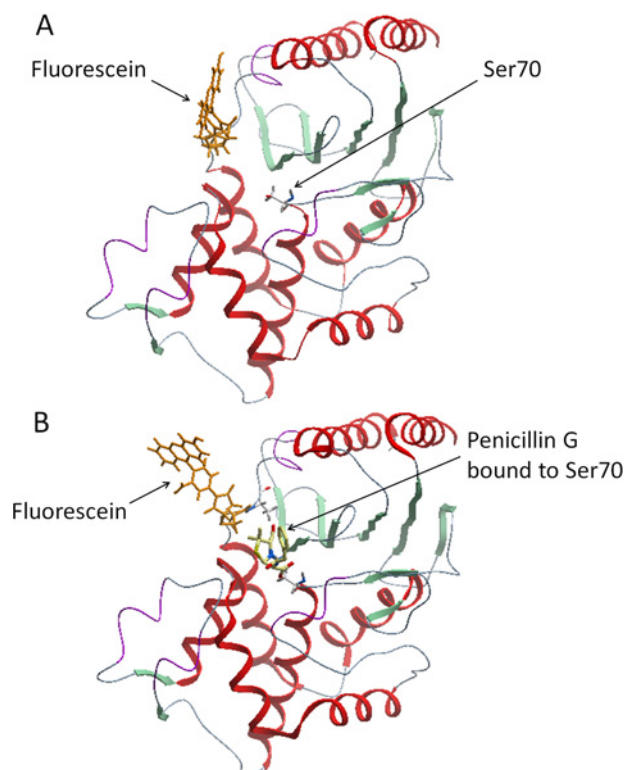


**Figure 6 Molecular models of the fluorescein-labelled TEM-1 V216C mutant in the free-enzyme (E) and  $ES^*$  states**

(A) Without penicillin G, the fluorescein molecule (orange) lies close to the active site of the enzyme. (B) With penicillin G, the fluorescein molecule (orange) stays away from the active site when penicillin G (yellow) binds to  $Ser^{70}$  in the active site. The ribbon diagrams represent the structure of the TEM-1 V216C mutant.

we conducted molecular modelling on the free enzyme (E) and  $ES^*$  states of the labelled V216C mutant with penicillin G as the substrate. Figure 6 shows the molecular models of the labelled V216C mutant with and without binding to penicillin G. In the free-enzyme state, the fluorescein molecule lies close to the active site (Figure 6A). Upon binding to penicillin G, the fluorescein molecule stays away from the active site (Figure 6B). This subtle conformational change is likely to keep the fluorescein molecule away from the residues around the active site, thus reducing their fluorescence quenching on the fluorescein molecule.

We compared the fluorescence of the fluorescein molecule in the folded state of the labelled V216C mutant and its fragmented state after trypsin digestion. This comparative study can verify whether the fluorescein molecule fluoresces weakly when staying close to the active site of the enzyme (folded state) and gives stronger fluorescence when staying away from the active site (fragmented state). The digestion on the labelled V216C mutant by trypsin was first monitored by SDS/PAGE analysis. Supplementary Figure S10 (available at <http://www.bioscirep.org/bsr/034/bsr034e136add.htm>) shows the fluorescent image of the SDS/PAGE gel for the labelled V216C mutant before and after trypsin digestion. Before trypsin digestion, the labelled V216C mutant shows a green fluorescent



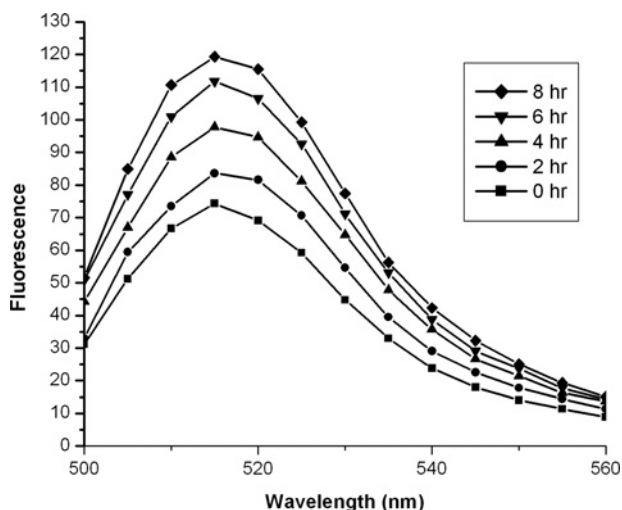


**Figure 7** Time-course fluorescence measurements on the labelled V216C mutant in the presence of trypsin

The fluorescence of the labelled V216C mutant increases in the course of trypsin digestion. The labelled V216C mutant ( $0.2 \text{ mg}\cdot\text{ml}^{-1}$ ) was mixed with trypsin ( $0.01 \text{ mg}\cdot\text{ml}^{-1}$ ) in 50 mM potassium phosphate buffer (pH 7.0).

band at the position corresponding to the undigested form (Figure S10). After incubation with trypsin for 8 h, some green fluorescent bands appear at lower positions, indicating that the labelled V216C mutant was cleaved into smaller peptide fragments by trypsin (Figure S10). We then examined the fluorescence of the labelled V216C mutant in response to trypsin digestion. Interestingly, the fluorescence of the labelled V216C mutant increases as a function of time during the course of trypsin digestion (Figure 7). This experimental observation implies that the fluorescein molecule is likely to experience fluorescence quenching when it stays close to the enzyme's active site in the folded state. Such fluorescence quenching is relieved when the fluorescein molecule stays away from the active site as a result of the trypsin digestion on the structure of the labelled V216C mutant, thus leading to the fluorescence enhancement of the fluorescein molecule. Taking the results of the ESI-MS, molecular modelling and trypsin digestion studies together, the fluorescein molecule is likely to lie close to the active site in the free enzyme state (E) and fluoresces weakly due to fluorescence quenching by the residues around the active site. Upon binding to  $\beta$ -lactam antibiotics, the fluorescein molecule is likely to stay away from the active site and experience weaker fluorescence quenching, thus giving stronger fluorescence in the substrate-bound state (ES and ES\*). After enzymatic hydrolysis, the hydrolysed product (P) will be released from the active site, and therefore the fluorescein molecule will approach the active site again and restore its weak fluorescence.

## Conclusions

In summary, we have discovered that the Val<sup>216</sup> residue in TEM-1 is a good site for the replacement with a cysteine and subsequent

fluorophore labelling at Cys<sup>216</sup> for the construction of a fluorescent drug sensor for *in vitro* drug screening. The labelled TEM-1 V216C mutant is catalytically active compared with the wild-type enzyme and can distinguish drug binders from non-binders and 'drug aggregates' by giving characteristic fluorescence profiles. The labelled TEM-1 V216C mutant can also fluorescently differentiate between potent and impotent  $\beta$ -lactam antibiotics, highlighting its potential use in the development of new-generation  $\beta$ -lactam antibiotics. With its catalytically active nature and effective fluorescent drug-sensing function, the labelled TEM-1 V216C mutant can mimic its wild-type form as a molecular drug target for *in vitro* drug screening. More importantly, given the high conservation of Val<sup>216</sup> in the members of the TEM family, the combined strategy of Val<sup>216</sup>→Cys<sup>216</sup> mutation and fluorophore labelling at Cys<sup>216</sup> can be further extended to other clinically significant TEM variants (ESBL and IRT) for the construction of tailor-made *in vitro* drug screening tools. Such tools will greatly advance the drug discovery and development against clinically significant TEM-type  $\beta$ -lactamases. In this regard, the labelled TEM-type V216C mutants have the potential to act as high-throughput antibiotic screening tools against  $\beta$ -lactamase-producing bacteria with the aid of fluorescence microplate readers [41]. With  $\beta$ -lactamase-resistant antibiotics, the  $\beta$ -lactamase produced by bacteria will be inhibited, and therefore the labelled V216C mutant will receive intact antibiotics and give stronger fluorescence signals [41]. For  $\beta$ -lactamase-unstable antibiotics, they will be rapidly hydrolysed by the  $\beta$ -lactamase from bacteria, and therefore the labelled V216C mutant will be depleted of intact antibiotics and give much weaker fluorescence signals [41]. In addition to this drug screening function against antibiotic-resistant bacteria, the labelled TEM-type V216C mutants can mimic their wild-type forms to provide insights into the potency of new  $\beta$ -lactam antibiotics and their inactivation mechanisms by exhibiting characteristic fluorescence profiles [20]; the increasing and decreasing time-course fluorescence signals indicate the formation of ES\* complex through acylation and the restoration of free enzyme (E) through deacylation, respectively [20]. The use of such fluorescence profiles will facilitate the design of new  $\beta$ -lactam antibiotics and  $\beta$ -lactamase inhibitors with stronger potency.

## AUTHOR CONTRIBUTION

Wing-Lam Cheong did the protein expression and purification, fluorescence assays, and enzyme kinetic studies. Ming-San Tsang was responsible for the preparation of the TEM-1 V216C mutant. Piu-Kin So and Wai-Hong Chung conducted ESI-MS and molecular modelling studies, respectively. Yun-Chung Leung and Pak-Ho Chan were responsible for the project design.

## FUNDING

We thank the National Natural Science Foundation of China [grant number 21205101], the Hong Kong, Macao and Taiwan Science & Technology Cooperation Programme of China [grant number 2013DFH30070], the State Key Laboratory of Chirosciences [grant number 4-BBX3], the Matching Fund of the Shenzhen Government



(People's Republic of China) and the Research Committee of the Hong Kong Polytechnic University for support to this project.

## REFERENCES

- McDonough, M. A., Anderson, J. W., Silvaggi, N. R., Pratt, R. F., Knox, J. R. and Kelly, J. A. (2002) Structures of two kinetic intermediates reveal species specificity of penicillin-binding proteins. *J. Mol. Biol.* **322**, 111–122 [CrossRef PubMed](#)
- Fisher, J. F., Meroueh, S. O. and Mobashery, S. (2005) Bacterial resistance to  $\beta$ -lactam antibiotics: compelling opportunism, compelling opportunity. *Chem. Rev.* **105**, 395–424 [CrossRef PubMed](#)
- Matagne, A., Dubus, A., Galleni, M. and Frere, J. M. (1999) The  $\beta$ -lactamase cycle: a tale of selective pressure and bacterial ingenuity. *Nat. Prod. Rep.* **16**, 1–19 [CrossRef PubMed](#)
- Sandanayaka, V. P. and Prasad, A. S. (2002) Resistance to  $\beta$ -lactam antibiotics: structure and mechanism based design of  $\beta$ -lactamase inhibitors. *Curr. Med. Chem.* **9**, 1145–1165 [CrossRef PubMed](#)
- Livermore, D. M. (1995)  $\beta$ -lactamases in laboratory and clinical resistance. *Clin. Microbiol. Rev.* **8**, 557–584 [PubMed](#)
- Bradford, P. A. (2001) Extended-spectrum  $\beta$ -lactamases in the 21st century: characterization, epidemiology, and detection of this important resistance threat. *Clin. Microbiol. Rev.* **14**, 933–951 [CrossRef PubMed](#)
- Matagne, A., Lamotte-Brasseur, J. and Frere, J. M. (1998) Catalytic properties of class A  $\beta$ -lactamases: efficiency and diversity. *Biochem. J.* **330**, 581–598 [PubMed](#)
- Chaibi, E. B., Sirot, D., Paul, G. and Labia, R. (1999) Inhibitor-resistant TEM  $\beta$ -lactamases: phenotypic, genetic and biochemical characteristics. *J. Antimicrob. Chemother.* **43**, 447–458 [CrossRef PubMed](#)
- Paterson, D. L. and Bonomo, R. A. (2005) Extended-spectrum  $\beta$ -lactamases: a clinical update. *Clin. Microbiol. Rev.* **18**, 657–686 [CrossRef PubMed](#)
- Hawkey, P. M. (2008) Prevalence and clonality of extended-spectrum  $\beta$ -lactamases in Asia. *Clin. Microbiol. Infect.* **14**, 159–165 [CrossRef PubMed](#)
- Bush, K. (2013) The ABCD's of  $\beta$ -lactamase nomenclature. *J. Infect. Chemother.* **19**, 549–559 [CrossRef PubMed](#)
- Watkins, R. R., Papp-Wallace, K. M., Drawz, S. M. and Bonomo, R. A. (2013) Novel  $\beta$ -lactamase inhibitors: a therapeutic hope against the scourge of multidrug resistance. *Front. Microbiol.* **4**, 1–8 [CrossRef PubMed](#)
- Abagyan, R. and Totrov, M. (2001) High-throughput docking for lead generation. *Curr. Opin. Chem. Biol.* **5**, 375–382 [CrossRef PubMed](#)
- Powers, R. A., Morandi, F. and Shoichet, B. K. (2002) Structure-based discovery of a novel, noncovalent inhibitor of AmpC  $\beta$ -lactamase. *Structure* **10**, 1013–1023 [CrossRef PubMed](#)
- Kitchen, D. B., Decornez, H., Furr, J. R. and Bajorath, J. (2004) Docking and scoring in virtual screening for drug discovery: methods and applications. *Nat. Rev. Drug Discov.* **3**, 935–949 [CrossRef PubMed](#)
- Schuttelkopf, A. W. and van Aalten, D. M. F. (2004) PRODRG: a tool for high-throughput crystallography of protein–ligand complexes. *Acta Crystallogr. D* **60**, 1355–1363 [CrossRef](#)
- Babaoglu, K., Simeonov, A., Lwin, J. J., Nelson, M. E., Feng, B., Thomas, C. J., Cancian, L., Costi, M. P., Maltby, D. A., Jadhav, A. et al. (2008) Comprehensive mechanistic analysis of hits from high-throughput and docking screens against  $\beta$ -lactamase. *J. Med. Chem.* **51**, 2502–2511 [CrossRef PubMed](#)
- Coan, K. E. D., Maltby, D. A., Burlingame, A. L. and Shoichet, B. K. (2009) Promiscuous aggregate-based inhibitors promote enzyme unfolding. *J. Med. Chem.* **52**, 2067–2075 [CrossRef PubMed](#)
- O'callaghan, Ch, Shingler, A. H., Kirby, S. M. and Morris, A. (1972) Novel method for detection of  $\beta$ -lactamases by using a chromogenic cephalosporin substrate. *Antimicrob. Agents Chemother.* **1**, 283–288 [CrossRef PubMed](#)
- Chan, P. H., So, P. K., Ma, D. L., Zhao, Y., Lai, T. S., Chung, W. H., Chan, K. C., Yiu, K. F., Chan, H. W., Siu, F. M. et al. (2008) Fluorophore-labeled  $\beta$ -lactamase as a biosensor for  $\beta$ -lactam antibiotics: a study of the biosensing process. *J. Am. Chem. Soc.* **130**, 6351–6361 [CrossRef PubMed](#)
- Chan, P. H., Liu, H. B., Chen, Y. W., Chan, K. C., Tsang, C. W., Leung, Y. C. and Wong, K. Y. (2004) Rational design of a novel fluorescent biosensor for  $\beta$ -lactam antibiotics from a class A  $\beta$ -lactamase. *J. Am. Chem. Soc.* **126**, 4074–4075 [CrossRef PubMed](#)
- Benson, D. E., Conrad, D. W., de Lorimer, R. M., Trammell, S. A. and Hellinga, H. W. (2001) Design of bioelectronic interfaces by exploiting hinge-bending motions in proteins. *Science* **293**, 1641–1644 [CrossRef PubMed](#)
- Salins, L. L. E., Goldsmith, E. S., Ensor, C. M. and Daunert, S. (2002) A fluorescence-based sensing system for the environmental monitoring of nickel using the nickel binding protein from *Escherichia coli*. *Anal. Bioanal. Chem.* **372**, 174–180 [CrossRef PubMed](#)
- Shrestha, S., Salins, L. L. E., Ensor, C. M. and Daunert, S. (2002) Rationally designed fluorescently labeled sulfate-binding protein mutants: evaluation in the development of a sensing system for sulfate. *Biotechnol. Bioeng.* **78**, 517–526 [CrossRef PubMed](#)
- Lager, I., Fehr, M., Frommer, W. B. and Lalonde, S. W. (2003) Development of a fluorescent nanosensor for ribose. *FEBS Lett.* **553**, 85–89 [CrossRef PubMed](#)
- Ye, K. M. and Schultz, J. S. (2003) Genetic engineering of an allosterically based glucose indicator protein for continuous glucose monitoring by fluorescence resonance energy transfer. *Anal. Chem.* **75**, 3451–3459 [CrossRef PubMed](#)
- Leung, Y. C., Robinson, C. V., Aplin, R. T. and Waley, S. G. (1994) Site-directed mutagenesis of  $\beta$ -lactamase I: role of Glu166. *Biochem. J.* **299**, 671–678 [PubMed](#)
- Waley, S. G. (1974) A spectrophotometric assay of  $\beta$ -lactamase action on penicillins. *Biochem. J.* **139**, 789–790 [PubMed](#)
- Minami, S., Yotsuji, A., Inoue, M. and Mitsushashi, S. (1980) Induction of  $\beta$ -lactamase by various  $\beta$ -lactam antibiotics in *Enterobacter Cloacae*. *Antimicrob. Agents Chemother.* **18**, 382–385 [CrossRef PubMed](#)
- Adachi, H., Ohta, T. and Matsuzawa, H. (1991) Site-directed mutants, at position 166, of RTEM-1  $\beta$ -lactamase that form a stable acyl-enzyme intermediate with penicillin. *J. Biol. Chem.* **266**, 3186–3191 [PubMed](#)
- Sawai, T. and Tsukamoto, K. (1982) Cefoxitin, N-formimidoyl thienamycin, clavulanic acid, and penicillanic acid sulfone as suicide inhibitors for different types of  $\beta$ -lactamases produced by Gram-negative bacteria. *J. Antibiot.* **35**, 1594–1602 [CrossRef PubMed](#)
- Livermore, D. M. (1998)  $\beta$ -Lactamase-mediated resistance and opportunities for its control. *J. Antimicrob. Chemother.* **41**, 25–41 [CrossRef PubMed](#)
- Fisher, J., Belasco, J. G., Khosla, S. and Knowles, J. R. (1980)  $\beta$ -Lactamase proceeds via an acyl-enzyme intermediate. Interaction of the *Escherichia coli* RTEM enzyme with cefoxitin. *Biochemistry* **19**, 2895–2901 [CrossRef PubMed](#)

- 34 Reading, C. and Farmer, T. (1981) The inhibition of  $\beta$ -lactamases from Gram-negative bacteria by clavulanic acid. *Biochem. J.* **199**, 779–787 [PubMed](#)
- 35 Imtiaz, U., Billings, E., Knox, J. R., Manavathu, E. K., Lerner, S. A. and Mobashery, S. (1993) Inactivation of class A  $\beta$ -lactamases by clavulanic acid: the role of arginine-244 in a proposed nonconcerted sequence of events. *J. Am. Chem. Soc.* **115**, 4435–4442 [CrossRef](#)
- 36 McGovern, S. L., Helfand, B. T., Feng, B. and Shoichet, B. K. (2003) A specific mechanism of nonspecific inhibition. *J. Med. Chem.* **46**, 4265–4272 [CrossRef PubMed](#)
- 37 McGovern, S. L. and Shoichet, B. K. (2003) Kinase inhibitors: not just for kinases anymore. *J. Med. Chem.* **46**, 1478–1483 [CrossRef PubMed](#)
- 38 Seidler, J., McGovern, S. L., Doman, T. N. and Shoichet, B. K. (2003) Identification and prediction of promiscuous aggregating inhibitors among known drugs. *J. Med. Chem.* **46**, 4477–4486 [CrossRef PubMed](#)
- 39 McGovern, S. L., Caselli, E., Grigorieff, N. and Shoichet, B. K. (2002) A common mechanism underlying promiscuous inhibitors from virtual and high-throughput screening. *J. Med. Chem.* **45**, 1712–1722 [CrossRef PubMed](#)
- 40 Bush, K. and Sykes, R. B. (1986) Methodology for the study of  $\beta$ -lactamases. *Antimicrob. Agents Chemother.* **30**, 6–10 [CrossRef PubMed](#)
- 41 Chan, P. H., Chan, K. C., Liu, H. B., Chung, W. H., Leung, Y. C. and Wong, K. Y. (2005) Fluorescein-labeled  $\beta$ -lactamase mutant for high-throughput screening of bacterial  $\beta$ -lactamases against  $\beta$ -lactam antibiotics. *Anal. Chem.* **77**, 5268–5276 [CrossRef PubMed](#)

---

Received 4 April 2014/7 July 2014; accepted 28 July 2014

Published as Immediate Publication 30 July 2014, doi 10.1042/BSR20140057

---



OPEN ACCESS

## SUPPLEMENTARY DATA

# Fluorescent TEM-1 $\beta$ -lactamase with wild-type activity as a rapid drug sensor for *in vitro* drug screening

Wing-Lam Cheong\*, Ming-San Tsang\*, Pui-Kin So\*, Wai-Hong Chung\*, Yun-Chung Leung\* and Pak-Ho Chan\*<sup>†1</sup>

\*State Key Laboratory of Chirosciences, Food Safety and Technology Research Centre, Department of Applied Biology and Chemical Technology, The Hong Kong Polytechnic University, Hung Hom, Kowloon, Hong Kong, People's Republic of China

<sup>†</sup>The Hong Kong Polytechnic University Shenzhen Research Institute, Shenzhen 518057, People's Republic of China

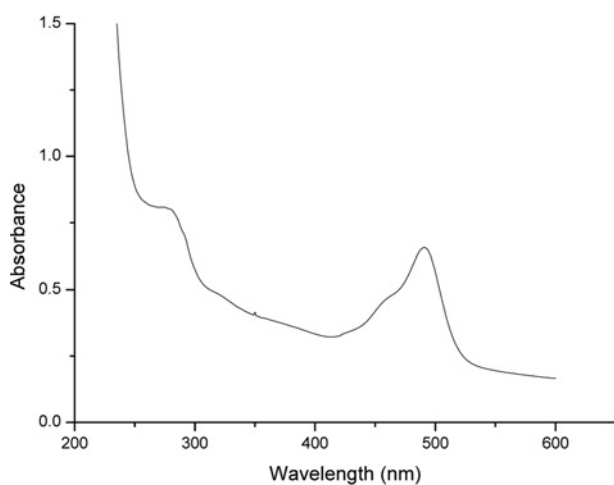


**Figure S1 UV/Vis absorption spectrum of the fluorescein-labelled V216C mutant in 50 mM potassium phosphate buffer (pH 7.0)**

[Labelled V216C] = 10  $\mu$ M.

<sup>1</sup> To whom correspondence should be addressed (email: pak-ho.chan@polyu.edu.hk).

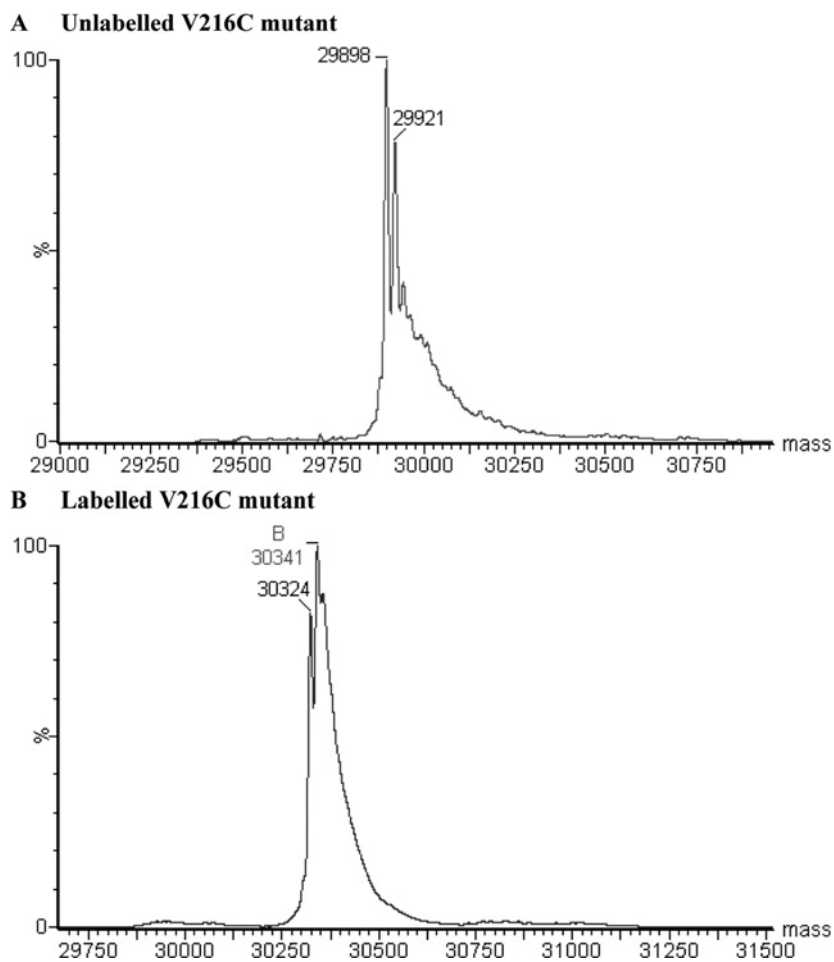


**Figure S2 ESI mass spectra of the TEM-1 V216C mutant with and without labelling with fluorescein-5-maleimide**  
(A) Mass spectrum of the V216C mutant without fluorophore labelling. The mass peaks of 29898 and 29921 kDa correspond to the V216C mutant and the [V216C + Na] adduct, respectively. (B) Mass spectrum of the V216C mutant with fluorophore labelling. The mass peaks of 30324 and 30341 Da correspond to the labelled V216C mutant and the [labelled V216C + H<sub>2</sub>O] adduct, respectively.

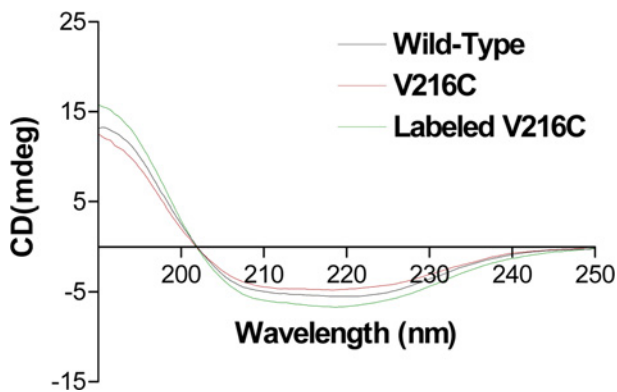


**Figure S3 Far-UV CD measurements of the wild-type and mutant forms of the TEM-1  $\beta$ -lactamase**

Far-UV CD signals: wild-type TEM-1 (black line), unlabelled V216C (red line) and labelled V216C (green line).

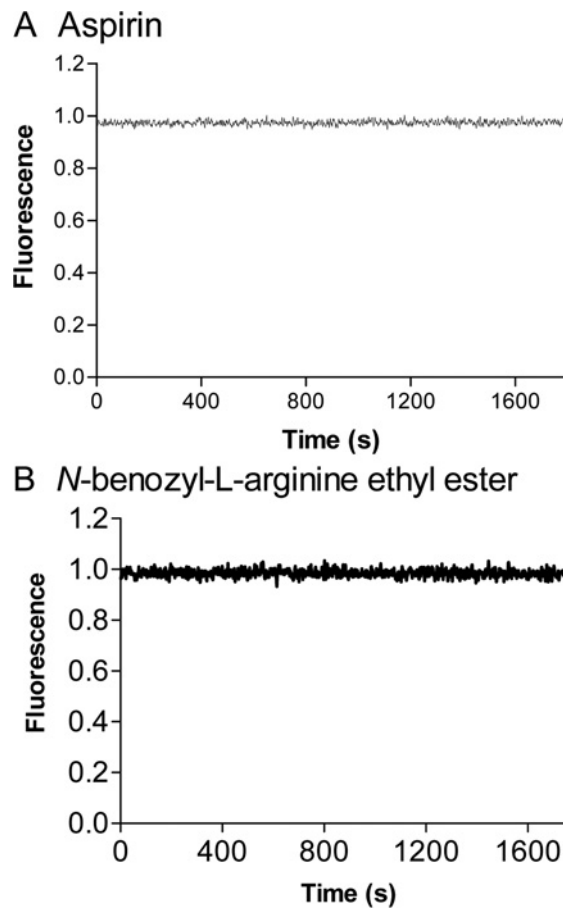


**Figure S4 Time-course fluorescence measurements of the labelled V216C mutant with non-binders**

(A) fluorescence signals of the labelled V216C mutant (20 nM) with 1 mM aspirin; (B) fluorescence signals of the labelled V216C mutant (20 nM) with 1 mM BAEE. Excitation: 494 nm. Buffer: 50 mM potassium phosphate (pH 7.0).

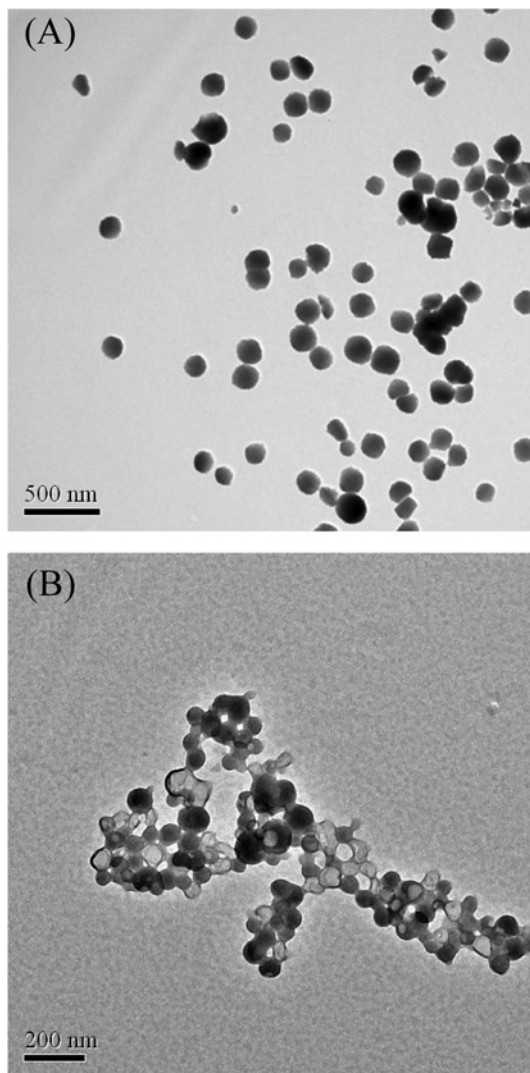


**Figure S5 Transmission electron microscopic images of (A) Congo red (10  $\mu$ M) and (B) TIPP (10  $\mu$ M) in the presence of the labelled V216C mutant (20 nM)**

Aggregates were formed by Congo red and TIPP under aqueous conditions.

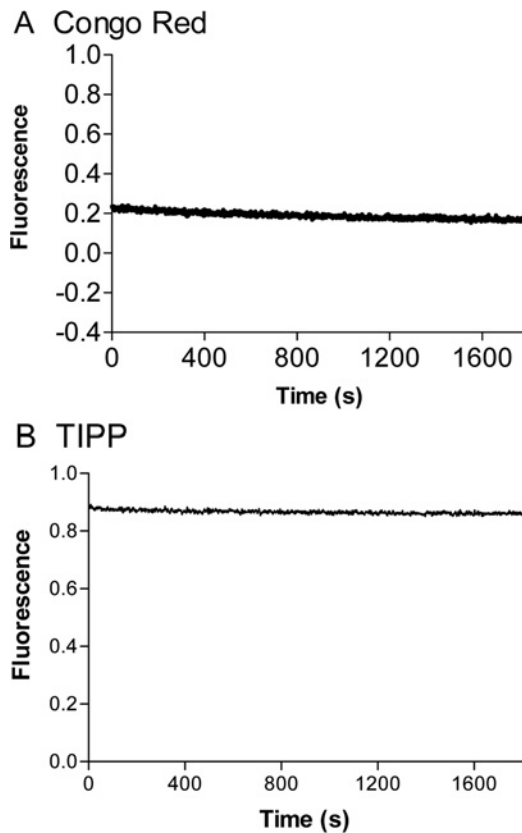


**Figure S6 Time-course fluorescence measurements of the labelled V216C mutant in the presence of 'drug aggregates'**

(A) fluorescence signals of the labelled V216C mutant (20 nM) in the presence of 10  $\mu$ M Congo red; (B) fluorescence signals of the labelled V216C mutant (20 nM) in the presence of 10  $\mu$ M TIPP. Buffer: 50 mM potassium phosphate (pH 7.0). Congo red and TIPP formed aggregates under such aqueous conditions (Figure S5).

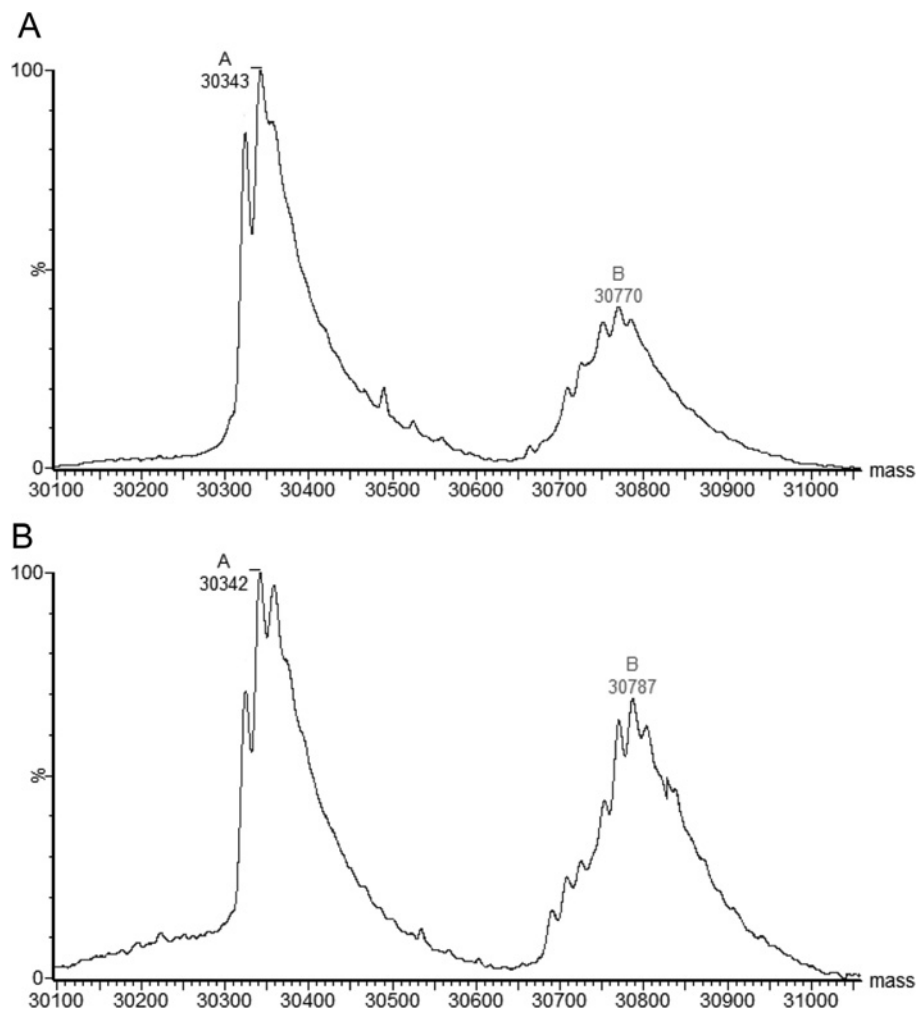


**Figure S7** ESI mass spectra of the labelled V216C mutant (5  $\mu$ M) with cefoxitin (10 mM) at various time intervals (A)  $t = 1$  min and (B)  $t = 10$  min. Buffer: 20 mM ammonium acetate solution (pH 7.0). Peaks A and B correspond to the labelled V216C mutant and the covalent labelled V216C-cefoxitin complex, respectively.



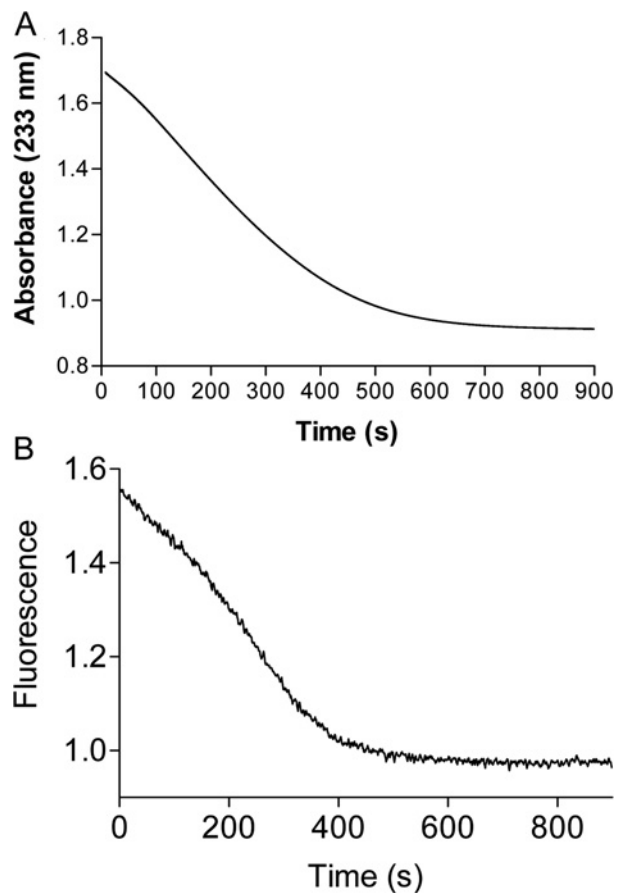


**Figure S8 Time-course fluorescence and UV absorbance measurements of the labelled V216C mutant with penicillin G**

(A) UV absorbance of penicillin G at different time intervals; (B) fluorescence signals of the labelled V216C mutant at different time intervals. [Labelled V216C] = 20 nM; [Penicillin G] = 1 mM. Buffer: 50 mM potassium phosphate buffer (pH 7.0).

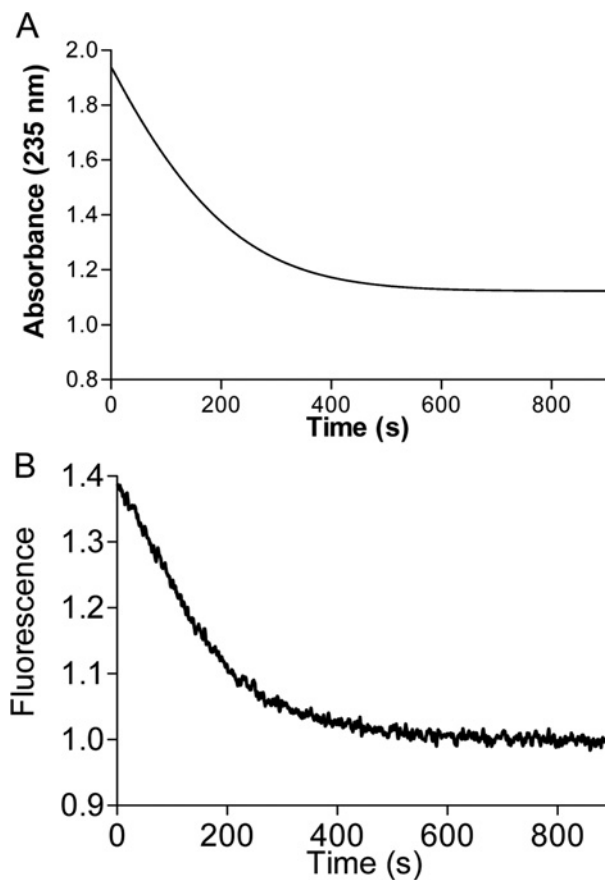


**Figure S9 Time-course fluorescence and UV absorbance measurements of the labelled V216C mutant with ampicillin**

(A) UV absorbance of ampicillin at different time intervals; (B) fluorescence signals of the labelled V216C mutant at different time intervals. [Labelled V216C] = 20 nM; [Ampicillin] = 1 mM. Buffer: 50 mM potassium phosphate buffer (pH 7.0).

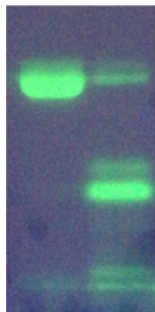


**Figure S10 SDS/PAGE analysis of the labelled V216C mutant with and without trypsin digestion**

The SDS/PAGE gel was illuminated with the UV light. (Left) the labelled V216C mutant without trypsin digestion; (Right) the labelled V216C mutant after trypsin digestion.

---

**Received 4 April 2014/7 July 2014; accepted 28 July 2014**

**Published as Immediate Publication 30 July 2014, doi 10.1042/BSR20140057**

---